



# Long non-coding RNA (LncRNA) non-coding RNA activated by DNA damage (NORAD) knockdown alleviates airway remodeling in asthma via regulating miR-410-3p/RCC2 and inhibiting Wnt/ $\beta$ -catenin pathway

Ting Zhang<sup>\*</sup>, Han Huang, Lihong Liang, Hongxia Lu, Dongge Liang

Department of Respiratory, Henan Children's Hospital, Zhengzhou Children's Hospital, Zhengzhou 450000, China

## ARTICLE INFO

### Keywords:

Long non-coding RNA NORAD  
Epithelial-mesenchymal transition  
asthma  
miR-410-3p/chromosome condensation 2  
Wnt/ $\beta$ -catenin

## ABSTRACT

**Background:** Asthma is a chronic inflammatory disorder with high prevalence in childhood. Airway remodeling, an important structural change of the airways, is resulted from epithelial-mesenchymal transition. Long non-coding RNA non-coding RNA activated by DNA damage (NORAD) has been found to promote epithelial-mesenchymal transition in multiple cancers. This study aimed to analyze the role of NORAD in asthma, mainly focusing on epithelial-mesenchymal transition-mediated airway remodeling, and further explored the NORAD-miRNA-mRNA network.

**Methods:** NORAD expression was analyzed in transforming growth factor- $\beta$ 1-induced BEAS-2B human bronchial epithelial cells and ovalbumin-challenged asthmatic mice. The influences of NORAD on the epithelial-mesenchymal transition characteristics and Wnt/ $\beta$ -catenin pathway activation were analyzed *in vitro*. The interactions between NORAD and miR-410-3p as well as miR-410-3p and regulator of chromosome condensation 2 were detected by dual-luciferase reporter assay and RNA pull-down assay. Rescue experiments using miR-410-3p antagonist and chromosome condensation 2 overexpression were used to confirm the mechanism of NORAD. Additionally, the role and mechanism of NORAD were further evaluated in asthmatic mice.

**Results:** NORAD expression was elevated in both asthmatic models. Knockdown of NORAD impeded spindle-like morphology changes, elevated E-cadherin expression, decreased N-cadherin expression, suppressed cell migration, and inactivated the Wnt/ $\beta$ -catenin pathway in transforming growth factor- $\beta$ 1-stimulated BEAS-2B cells. NORAD acted as a sponge of miR-410-3p to regulate chromosome condensation 2 expression. Rescue assays demonstrated that silencing of NORAD ameliorated transforming growth factor- $\beta$ 1-induced EMT via miR-410-3p/chromosome condensation 2/Wnt/ $\beta$ -catenin axis. *In vivo*, knockdown of NORAD led to the reduction of inflammatory cell infiltration and collagen deposition, suppression of IL-4, IL-13, transforming growth factor- $\beta$ 1 and immunoglobulin E production, decreasing of N-cadherin, chromosome condensation 2,  $\beta$ -catenin and c-Myc expression, but increasing of E-cadherin and miR-410-3p expression.

**Conclusions:** Silencing of NORAD alleviated epithelial-mesenchymal transition-mediated airway remodeling in asthma via mediating miR-410-3p/chromosome condensation 2/Wnt/ $\beta$ -catenin pathway.

<sup>\*</sup> Corresponding author. No. 255 Nanyang Road, Gangdu Street, Zhengzhou 450000, Henan Province, China.  
E-mail address: [18739930036@163.com](mailto:18739930036@163.com) (T. Zhang).

<https://doi.org/10.1016/j.heliyon.2023.e23860>

Received 28 February 2023; Received in revised form 14 December 2023; Accepted 14 December 2023

Available online 15 December 2023

2405-8440/© 2023 Published by Elsevier Ltd.

This is an open access article under the CC BY-NC-ND license

(<http://creativecommons.org/licenses/by-nc-nd/4.0/>).

## 1. Introduction

Asthma is a chronic inflammatory disease of the airways that may result from exposure to allergens or other environmental irritants. Its typical feature is variable airway obstruction, leading to dyspnea, cough, wheezing, and chest tightness [1,2]. Asthma affects about 334 million people worldwide, leading to 250,000 annual deaths [3]. The prevalence of this disease in childhood is common, affecting approximately 14 % of children [4]. Asthmatic symptoms are presented before 3-year-old in about one-half of diagnosed-children [5]. Worryingly, the incidence of asthma is stable or decreasing in some developed countries, but it is increasing in developing countries [6]. In both children and adults, asthma can cause disability, low quality of life and deaths, which place a heavy burden on their patients, family and society [6]. Currently, inhaled corticosteroids are the most effective methods to control asthma; however, different subjects exhibit diverse responses to these therapies. Besides, the drugs reveal many adverse effects in asthmatic patients [7,8]. Hence, it is necessary to investigate new methods to treat asthma.

Through impacting on a variety of immune cells, epithelial cells and airway smooth muscle cells, asthma causes airway inflammation, airway hyper-responsiveness (AHR), mucus hypersecretion, subepithelial fibrosis, and airway remodeling [2]. Among them, airway inflammation and remodeling are two fundamental pathological features of asthma [9]. Airway remodeling is characterized by structural alterations of the airways, including airway wall thickening, subepithelial collagen deposition, and inflammatory cell infiltration [1,10]. Airway remodeling has been demonstrated to occur at early stage of disease progression and contribute to the severity of asthma [10]. Studies have shown that preventing airway remodeling at early stage potentially suppresses disease progression and improves control of asthma [11]. Epithelial-mesenchymal transition (EMT) can promote the differentiation of airway epithelia into myofibroblasts, accompanied by decreasing expression of epithelial biomarkers such as E-cadherin, whereas increasing expression of mesenchymal markers, such as N-cadherin. Accumulating evidence has demonstrated that dysregulation of EMT contributes to airway remodeling in asthma [12,13]. Therefore, reversing EMT process has become a crucial strategy to prevent airway remodeling.

Long non-coding RNAs (lncRNAs), the RNA transcripts with more than 200 nucleotides in length, have been demonstrated to be associated with asthma and function as key regulators in airway remodeling [14]. The expression of serum lncRNA KCNQ1 opposite strand/antisense transcript 1 was higher in bronchial asthmatic children with airway remodeling than non-remodeling. And in children with airway remodeling, serum lncRNA KCNQ1 opposite strand/antisense transcript 1 expression was related to the number of fibroblasts [15]. Huang et al. [16] found that lncRNA taurine upregulated gene 1 promoted airway remodeling and EMT in asthmatic mice. Non-coding RNA activated by DNA damage (NORAD) was a highly conserved mammalian lncRNA that directly mediated ploidy and chromosomal stability by sequestering PUMILIO proteins [17]. It has been reported to act as an oncogene in cancers like pancreatic and prostate cancers by modulating EMT [18–20]. However, the role of NORAD in the pathogenesis of asthma especially in airway remodeling is unclear.

Considering the vital role of NORAD in EMT as well as EMT in asthma, we speculated that NORAD might be involved in asthma. In this study, we investigated whether NORAD could promote airway remodeling in asthma. Transforming growth factor- $\beta$ 1 (TGF- $\beta$ 1) is a growth factor secreted by a variety of cells including airway epithelial cells and immune cells to induce EMT in asthma [21]. Hence, the effects of NORAD were analyzed in TGF- $\beta$ 1-induced BEAS-2B human bronchial epithelial cells and ovalbumin (OVA)-challenged asthmatic mice, respectively. Studies have demonstrated that lncRNAs function via the lncRNA-miRNA-mRNA competing endogenous RNA (ceRNA) network, in which lncRNAs can regulate gene expression by binding to specific miRNAs [22,23]. Hence, the underlying mechanism of NORAD in airway remodeling was explored focusing on the lncRNA-miRNA-mRNA network both *in vitro* and *in vivo*.

## 2. Materials and methods

### 2.1. Cell culture and treatment

BEAS-2B cells were purchased from American Tissue Culture Collection (ATCC, Manassas, VA, USA). They were grown in complete Bronchial Epithelial Cell Growth Medium (Lonza Clonetics, MD, USA), which contains bronchial epithelial cell growth basal medium and all the recommended supplements and growth factors, in a CO<sub>2</sub> incubator (5 %) at 37 °C. To induce EMT, BEAS-2B cells were stimulated with 10 ng/mL of TGF- $\beta$ 1 (Sigma-Aldrich, Louis, MO, USA) in complete Bronchial Epithelial Cell Growth Medium for 24 h as previously described [24].

### 2.2. Plasmid construction and cell transfection

Three short hairpin RNAs (shRNAs) targeting NORAD synthesized by GenePharma (Shanghai, China) were inserted into the pLVX-shRNA2-Puro plasmid to generate NORAD shRNA plasmids. The target sequences were as follows: sh#1: GTGTATATAA-TATGAAAAAGCTGCTCTCA; sh#2: GTTTAGAAGTGCACAAAGTATGTAAAAAG; sh#3: TATTAAAGAGTTGCCAATGTATGACA. The interfering efficiencies were analyzed by quantitative real-time PCR (qRT-PCR). And the most efficient one was transfected into human embryonic kidney 293T cells with other virus packaging plasmids (pMDLg pRRE, pRSV-rev and pCMV-VSV-G) to produce NORAD silencing lentivirus. For regulator of chromosome condensation 2 (RCC2) overexpression, RCC2 cDNA, which was amplified from BEAS-2B cells, was cloned into the pcDNA3.1 mammalian expression vector. The transfection efficiency was validated by Western blot analysis. All cell transfection protocols used Lipofectamine 3000 reagent (Invitrogen, Waltham, MA, USA) as the manufacturer's instructions.

In addition, NORAD cDNA fragments and the 3' untranslated regions segments of RCC2 containing miR-410-3p binding sites were amplified by PCR and inserted into the pGL3 luciferase promoter vector to construct NORAD (NORAD-Wt) and RCC2 (RCC2-Wt) wild type vectors. Also, their mutants obtained by mutating the binding sites were subcloned into the pGL3 plasmid to generate NORAD-Mut and RCC2-Mut vectors.

### 2.3. Dual luciferase reporter assay

BEAS-2B cells were planted into 24-well plates ( $3 \times 10^5$  cells/well). 24 h later, cells were transfected with 100 ng constructed luciferase vectors and 50 nM miR-410-3p mimic using Lipofectamine 3000 reagent. After incubation at 37 °C for 48 h, the relative luciferase activity was analyzed using the Dual-Luciferase Reporter Assay System (Promega, Madison, WI, USA).

### 2.4. Migration assay

The migration of BEAS-2B cells was investigated by Transwell chamber (8- $\mu$ m pore size; Millipore, Billerica, MA, USA).  $1 \times 10^5$  cells cultured in 200  $\mu$ L serum-free medium, which was bronchial epithelial cell growth basal medium that did not contain fetal bovine serum (FBS), were seeded on the upper chambers. And medium containing 10 % FBS (Hyclone, Logan, Utah, USA) and 10 ng/mL TGF- $\beta$ 1 was added to the lower chambers. After 24 h incubation at 37 °C, non-migrated cells were wiped out by a cotton tip, and migrated cells on the lower surface were fixed with methanol for 30 min, followed by staining with 0.1 % crystal violet for 20 min. Lastly, images were taken under an inverted microscope (Olympus, Tokyo, Japan). The number of migrated cells was counted from six randomly selected fields.

### 2.5. Cell viability analysis

Cell viability was detected by Cell Counting Kit-8 (CCK-8) kit (Beyotime, Shanghai, China). After transfection with or without designated plasmid for 24 h, BEAS-2B cells were seeded into 96-well plates with 5000 cells/well in 100  $\mu$ L of complete Bronchial Epithelial Cell Growth Medium. After stimulation with 10 ng/mL TGF- $\beta$ 1 for 24 h, 10  $\mu$ L of CCK-8 solution was added into each well and incubated for an additional 2 h at 37 °C. Then, the absorbance value of each well at 450 nm was measured using a microplate reader (Multiskan FC, Thermo Fisher Scientific, Waltham, MA, USA).

### 2.6. RNA pull-down assay

The RNA pull-down assay was performed with biotinylated miRNA. The biotinylated miR-410-3p and its mutant as well as a control RNA were synthesized by RiboBio (Guangzhou, China). They were transfected into BEAS-2B cells at a final concentration of 100 nM. 48 h after transfection, cells were collected and sonicated. Then, the cell lysates were incubated with streptavidin-coated magnetic beads (Promega) at 4 °C for 6 h. After washing with wash buffer, RNA mix bound to the bead was extracted with Trizol (Invitrogen). The contents of NORAD and RCC2 in the bound fraction were further quantified by qRT-PCR.

### 2.7. OVA-induced asthmatic model and interventions

Six-week-old female BALB/c mice were purchased from Charles River (Beijing, China) and the experiments were started after a week of adjustable feeding. During the experiments, all mice were allowed ad libitum access to food and water. All animal experiments were approved by the Animal Care and Use Committee of Henan Children's Hospital (Approval Number: 2021-002). Mice were randomly divided into 4 groups ( $n = 5$  per group): control, OVA, OVA + sh-NC, OVA + sh-NORAD. OVA was used to induce allergic asthma as previously described [13,25]. Briefly, mice were sensitized by intraperitoneal injection of 100  $\mu$ g OVA emulsified in 2 mg of aluminum hydroxide (Sigma-Aldrich) in 200  $\mu$ L PBS on days 0 and 7. The sensitized mice were intratracheally challenged with 100  $\mu$ g of OVA in 20  $\mu$ L of PBS on days 14, 17, and 20. Then, mice were challenged with OVA by intranasal administration twice a week for four weeks. And mice in the control group were sensitized and challenged with an equivalent amount of PBS. Under anaesthetization, NORAD shRNA or control lentiviral vectors ( $3 \times 10^6$  TU/mouse) were intratracheally delivered into mice 3 days before the first OVA challenge [26]. All mice were euthanized with 100 mg/kg pentobarbital sodium 24 h after the final challenge.

### 2.8. AHR analysis

AHR of mice were measured 24 h after the last challenge by the FlexiVent Pulmonary System (SCIREQ, Montreal, Quebec, Canada). After anaesthetization with 100 mg/kg pentobarbital sodium, the trachea of mouse was exposed and a cannula was inserted to delivery aerosol methacholine. Increasing concentrations of methacholine aerosol (2.5, 5, 10, 25, 50 mg/mL) were administered for 10 s. The airway resistance was monitored and recorded to evaluate AHR.

### 2.9. Histological staining

Lung tissues of mice were removed and fixed in 4 % neutral buffered formalin. After embedding in paraffin, samples were cut into 4- $\mu$ m thick sections. The slides were performed hematoxylin and eosin (HE) and Masson's trichrome staining to evaluate the

inflammatory severity and collagen content, respectively. And a semi-quantitative method was used to measure the peribronchial inflammation and subepithelial collagen deposition as described previously [27,28].

### 2.10. Enzyme-linked immunosorbent assay (ELISA)

Blood samples were collected by extirpating eyeballs before sacrificed. The serums were then obtained by centrifugating for 15 min at 10,000 g. Serum levels of total immunoglobulin E (IgE), interleukin (IL)-4, IL-13, and TGF- $\beta$ 1 were further assayed by ELISA kits from R&D Systems (Minnesota, USA) according to the manufacturer's instructions.

### 2.11. qRT-PCR analysis

All RNAs were extracted by TRIzol reagent. To detect mRNA expression, 500 ng of extracted RNA was reversely transcribed into cDNA using PrimeScript RT Reagent (TaKaRa, Japan). The qRT-PCR was carried out by Power SYBR Green PCR Master Mix (Applied Biosystems, UK), with GAPDH as an internal control. To analyze miR-410-3p expression, reverse-transcription and qRT-PCR processes were performed by TaqMan reverse transcription kit and TaqMan MicroRNA Assays (Thermo Fisher Scientific), U6 served as an internal control. Relative gene expression was calculated by using the  $2^{-\Delta\Delta Ct}$  method and primer sequences were exhibited in Table 1.

### 2.12. Western blot

Total protein was isolated from cells and lung tissues using RIPA Lysis Buffer (Beyotime). Protein concentrations were measured with a Bicinchoninic Acid protein assay kit (Beyotime). 30  $\mu$ g of proteins were separated by 12 % sodium dodecyl sulphate-polyacrylamide gel electrophoresis and transferred to polyvinylidene fluoride membranes. After saturating with 5 % non-fat milk for 2 h, the membranes were incubated with appropriate antibodies against E-cadherin (1:1000), N-cadherin (1:1500), RCC2 (1:1000), c-Myc (1:1000),  $\beta$ -actin (1:2000) (all were from Cell signaling technology, Danvers, MA, USA), and  $\beta$ -catenin (1:1200; Abcam, Cambridge, MA, USA) at 4 °C overnight, respectively. After washing with TBS-Tween (TBS + 0.05 % Tween 20), the membranes were probed with secondary antibody, which was conjugated with horseradish peroxidase. Protein bands were motivated by chemiluminescence (Millipore). The density of each band was quantified by Image J software, and the protein expression was normalized to  $\beta$ -actin.

### 2.13. Statistical analysis

Each experiment was carried out in three or five independent biological replicates, with three technical replicates in each. All data are shown as the mean  $\pm$  standard deviation (SD). Statistical analysis was performed by GraphPad Prism 5.0 (GraphPad Software, USA). Differences between two groups were analyzed by unpaired Student's t-test. Comparisons between three or more groups were detected by one-way analysis of variance (ANOVA) with Tukey test. *P* less than 0.05 was considered statistically significant.

## 3. Results

### 3.1. LncRNA NORAD is highly expressed in TGF- $\beta$ 1-induced bronchial epithelial cells

BEAS-2B cells were treated with 10 ng/mL of TGF- $\beta$ 1 for 24 h, and qRT-PCR assay was used for detecting the expression of NORAD. The results showed that there was an increase in NORAD expression in TGF- $\beta$ 1-treated cells when compared with the control (Fig. 1).

### 3.2. Knockdown of lncRNA NORAD inhibits TGF- $\beta$ 1-induced EMT characteristics in BEAS-2B cells

Three NORAD shRNA plasmids were constructed and their interfering efficiencies were analyzed. As indicated in Fig. 2A, sh#1

**Table 1**  
Primer sequences.

Gene	Forward (5' - 3')	Reverse (5' - 3')
Human NORAD	GTGACCACTCTGTCCGCAAT	AGAATGAAGACCAACCGCCC
Human RCC2	AAGGAGCGCGTCAAACCTTGAA	GCTTGCTGTTTAGGCACCTTCT
Human E-cadherin	CGAGAGCTACACGTTACGG	GGGTGTCGAGGGAAAAATAGG
Human N-cadherin	AGCCAACCTTAACTGAGGAGT	GGCAAGTTGATTGGAGGGATG
Human GAPDH	ACAACCTTGGTATCGTGGAAAG	GCCATCAGCCACAGTTTC
Mouse NORAD	TCGTTGTCTTTGGGGAGTGG	ACACACACTACATGGCCGGTT
Mouse RCC2	AAGGAGCGCGTCAAACCTTGAA	TGACCAAGGTTGCGGTACG
Mouse GAPDH	AGGTCGGTGTGAACGGATTG	GGGGTCGTTGATGGCAACA
miR-410-3p	ACACTCCAGCTGGGAATATAACACAGATG	TGGTGTCTGGAGTTCG
U6	CTCGCTTCGGCAGCAC	AACGCTTCACGAATTTGCGT

Note: NORAD: non-coding RNA activated by DNA damage; RCC2: chromosome condensation 2.

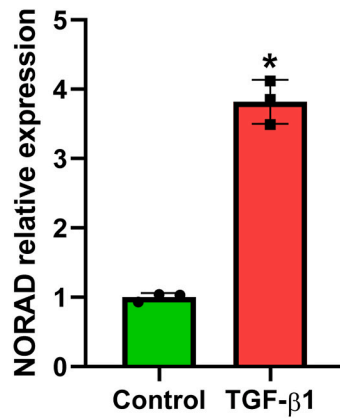


**Fig. 1.** LncRNA NORAD expression in TGF-β1-induced bronchial epithelial cells. BEAS-2B cells were stimulated with or without 10 ng/mL of TGF-β1, 24 h later, the expression of NORAD was detected by qRT-PCR. N = 3. \*P < 0.05, compared with the control group. NORAD: non-coding RNA activated by DNA damage; TGF-β1: transforming growth factor-β1; qRT-PCR: quantitative real-time PCR.

showed the highest efficacy among them and was used in the following study. The influence of NORAD on TGF-β1-induced EMT of BEAS-2B cells was evaluated by morphological analysis. Cells treated with 10 ng/mL TGF-β1 exhibited spindle-like morphology, while knockdown of NORAD successfully impeded such morphological changes (Fig. 2B). The EMT markers were also analyzed and the results demonstrated that TGF-β1 treatment significantly heightened the mRNA and protein expression levels of N-cadherin, but inhibited E-cadherin expression. These effects were alleviated after silencing of NORAD (Fig. 2C and D). Furthermore, EMT-like behavior, cell migration, was assayed by Transwell assay. As displayed in Fig. 2E, downregulation of NORAD markedly suppressed the migration of BEAS-2B cells induced by TGF-β1. Additionally, knockdown of NORAD remarkably inhibited TGF-β1-induced cell viability (Fig. 2F). These data suggested that downregulation of NORAD inhibited TGF-β1-induced EMT characteristics in BEAS-2B cells.

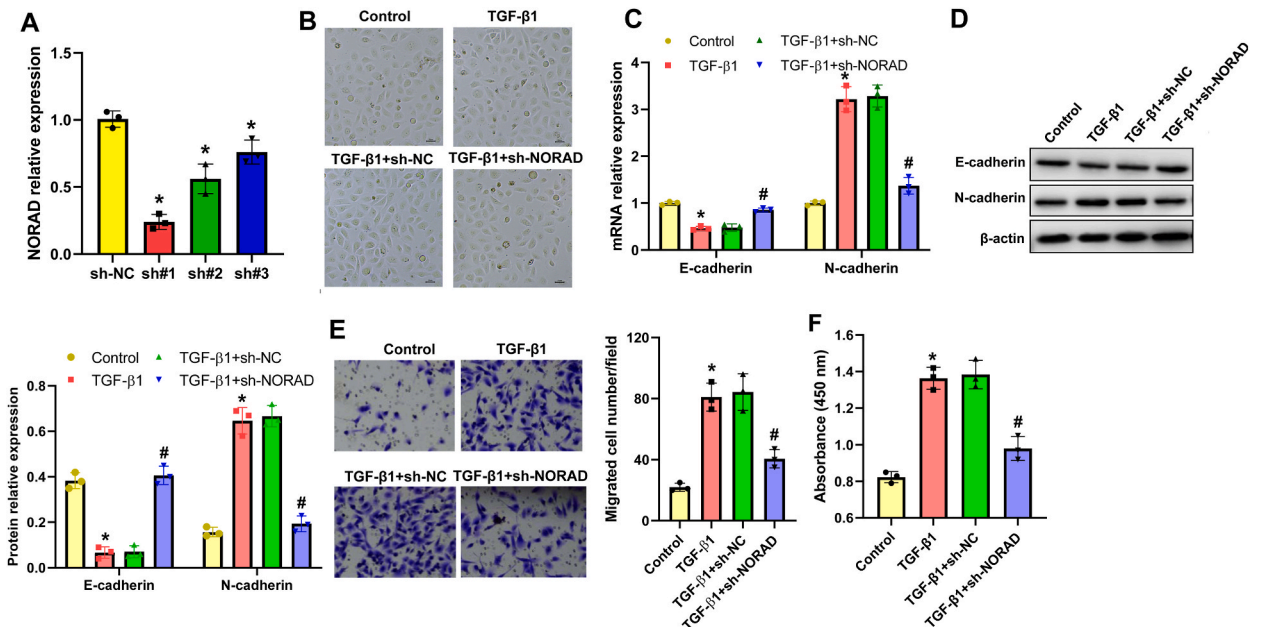


**Fig. 2.** LncRNA NORAD downregulation inhibited TGF-β1-induced EMT characteristics in BEAS-2B cells. A: BEAS-2B cells were transfected with three shRNAs targeting NORAD and the control sh-NC, the knockdown efficiency was analyzed by qRT-PCR. B: Cell morphology was taken by a microscope in BEAS-2B cells under different treatments. C: The mRNA levels of EMT markers, including E-cadherin and N-cadherin, were determined by qRT-PCR. D: Western blot assay for the protein levels of EMT markers. Non-adjusted images of Western blot analysis were presented in Supplemental Fig. S1. E: The migration of BEAS-2B cells was evaluated by Transwell assay. F: Cell viability was detected by CCK-8 assay. N = 3. \*P < 0.05, compared with the sh-NC group or control group. #P < 0.05, compared with the TGF-β1 group. NORAD: non-coding RNA activated by DNA damage; TGF-β1: transforming growth factor-β1; EMT: epithelial-mesenchymal transition; shRNA: short hairpin RNA; qRT-PCR: quantitative real-time PCR; CCK-8: cell counting kit-8.

### 3.3. LncRNA NORAD regulates EMT in BEAS-2B cells via miR-410-3p

LncRNA often serves as an endogenous miRNA sponge [29,30]. The potential binding miRNAs of NORAD were determined using Starbase software. MiR-410-3p was selected (Fig. 3A) because it has been demonstrated to attenuate airway inflammation in OVA-induced asthmatic mice and regulate the EMT process [31,32]. In TGF- $\beta$ 1-treated BEAS-2B cells, miR-410-3p expression was downregulated (Fig. 3B). Anti-miR-410-3p significantly enhanced TGF- $\beta$ 1-induced EMT and migration in BEAS-2B cells (Fig. 3C and D). Next, we further validated the interaction between NORAD and miR-410-3p by a luciferase reporter assay. The results revealed that miR-410-3p dramatically suppressed luciferase activities of BEAS-2B cells transfected with NORAD-Wt, but did not affect the luciferase activities of cells transfected with NORAD-Mut (Fig. 3E). Furthermore, RNA pull-down assay indicated that NORAD enrichment was elevated in biotin-miR-410-3p. Whereas, compared with the biotin-miR-410-3p group, NORAD was reduced in biotin-labeled mutant miR-410-3p group (Fig. 3F). Downregulation of NORAD elevated miR-410-3p expression, while miR-410-3p mimic did not affect the expression of NORAD (Fig. 3G and H). Additionally, our results revealed that compared with sh-NORAD transfected cells, the co-transfection of sh-NORAD and anti-miR-410-3p significantly promoted the EMT and migration of BEAS-2B cells (Fig. 3C and D). These results suggested that NORAD regulated EMT in BEAS-2B cells via directly interacting with miR-410-3p.

### 3.4. RCC2 is a target of miR-410-3p and lncRNA NORAD functions via mediating RCC2 in TGF- $\beta$ 1-induced BEAS-2B cells

We further investigated the target gene of miR-410-3p by searching Starbase online bioinformatic software and found that PITA, miRmap, miRanda, and TargetScan databases all predicted that RCC2 was a target gene of miR-410-3p and the binding sites between them were shown in Fig. 4A. TGF- $\beta$ 1 stimulation led to an increase of RCC2 expression in BEAS-2B cells (Fig. 4B and C). The luciferase assay demonstrated that miR-410-3p transfection decreased the luciferase reporter activities of RCC2-Wt, whereas showed no influence on the activities of RCC2-Mut (Fig. 4D). Also, compared with the bio-NC, there was an increase enrichment of RCC2 in biotin-miR-410-3p. A decrease of RCC2 enrichment in biotin-labeled mutant miR-410-3p was found when compared with the non-mutant one (Fig. 4E). The results indicated the sequence-specific binding of miR-410-3p to RCC2. RCC2 expression was inhibited by miR-410-3p in

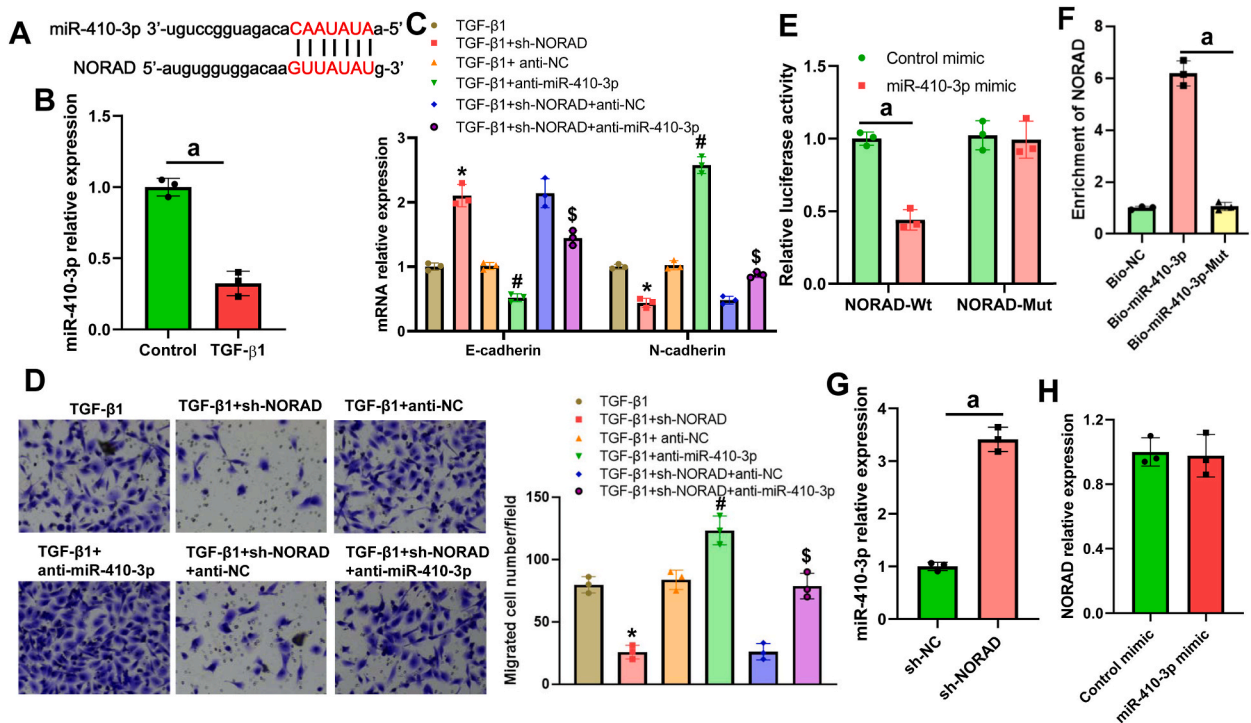


**Fig. 3.** LncRNA NORAD regulated EMT in BEAS-2B cells via miR-410-3p. **A:** The binding sites between NORAD and miR-410-3p predicted by Starbase. **B:** miR-410-3p expression was suppressed in BEAS-2B cells treated with 10 ng/mL TGF- $\beta$ 1. **C:** qRT-PCR was used to analyze the expression levels of E-cadherin and N-cadherin. **D:** The migration of BEAS-2B cells after designated treatments was assayed by Transwell method. **E:** Luciferase activities of BEAS-2B cells transfected with miR-410-3p/control mimic and NORAD-Wt/NORAD-Mut were measured. **F:** Biotin-labeled miRNA pull down assay for the direct binding of NORAD and miR-410-3p. **G:** miR-410-3p expression was increased in BEAS-2B cells transfected with sh-NORAD. **H:** NORAD level analyzed by qRT-PCR in BEAS-2B cells transfected with miR-410-3p mimic or control mimic.  $N = 3$ .  $^aP < 0.05$ ;  $^*P < 0.05$ , compared with the TGF- $\beta$ 1 group;  $^{\#}P < 0.05$ , compared with TGF- $\beta$ 1+anti-NC group;  $^{\$}P < 0.05$ , compared with TGF- $\beta$ 1+sh-NORAD + anti-NC group. NORAD: non-coding RNA activated by DNA damage; EMT: epithelial-mesenchymal transition; TGF- $\beta$ 1: transforming growth factor- $\beta$ 1; qRT-PCR: quantitative real-time PCR.

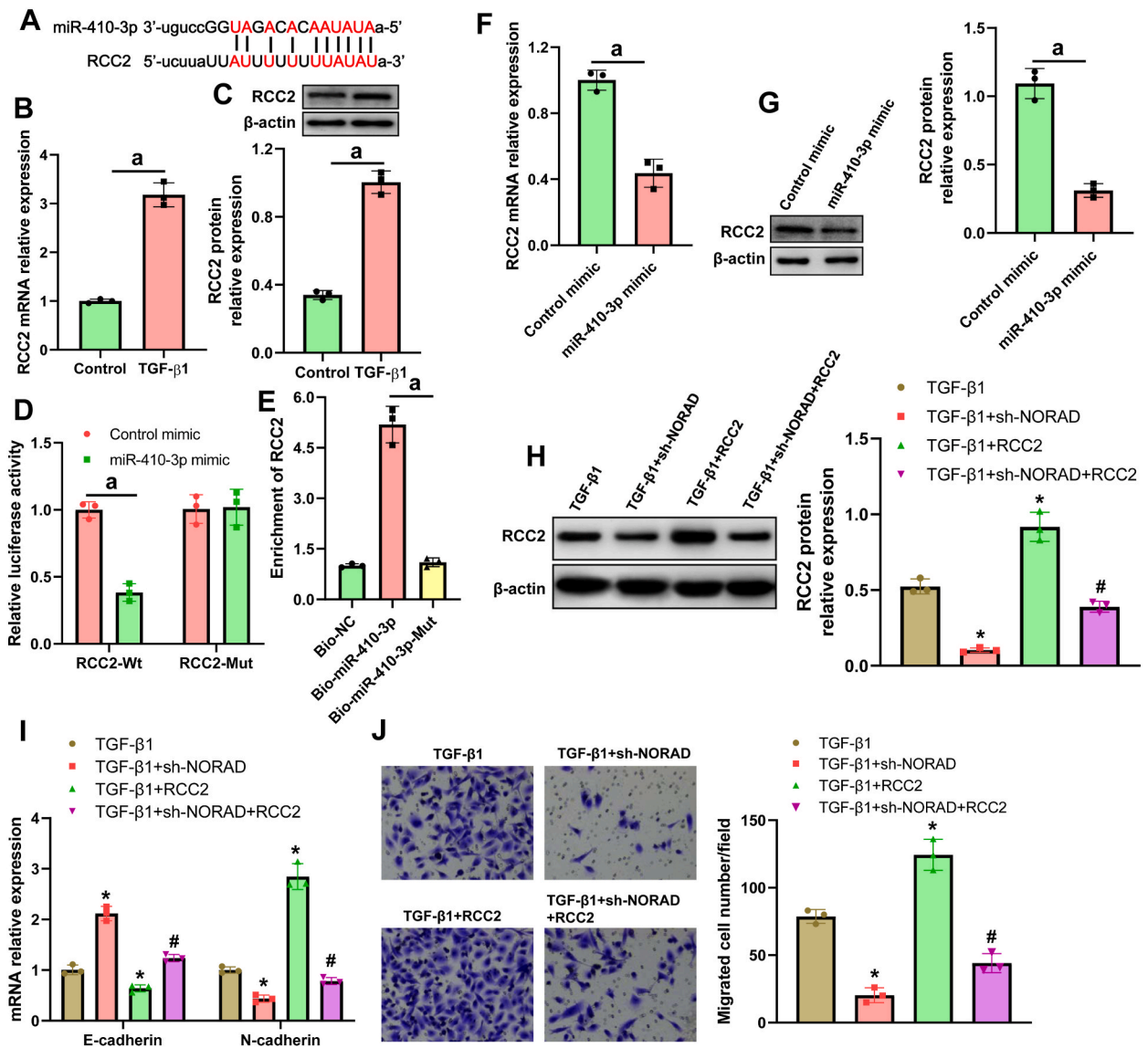


**Fig. 4.** LncRNA NORAD functioned via mediating RCC2 in TGF-β1-induced BEAS-2B cells. **A:** The binding sequence of miR-410-3p and RCC2. RCC2 mRNA (**B**) and protein (**C**) levels were both upregulated by TGF-β1 stimulation in BEAS-2B cells. Non-adjusted images of Western blot analysis were presented in [Supplemental Fig. S2](#). Luciferase (**D**) and biotin-labeled miRNA pull down assays (**E**) were used to analyze the relationship between miR-410-3p and RCC2. MiR-410-3p mimic decreased the mRNA (**F**) and protein (**G**) expression of RCC2 in TGF-β1-induced BEAS-2B cells. Non-adjusted images of Western blot analysis were presented in [Supplemental Fig. S2](#). **H:** RCC2 protein levels were detected by Western blot. Non-adjusted images of Western blot analysis were presented in [Supplemental Fig. S2](#). **I:** The expression of E-cadherin and N-cadherin in BEAS-2B cells. **J:** Transwell analysis for the migration of BEAS-2B cells under designated treatments. N = 3. <sup>a</sup>*P* < 0.05; <sup>\*</sup>*P* < 0.05, compared with the TGF-β1 group; <sup>#</sup>*P* < 0.05, compared with TGF-β1+sh-NORAD group. NORAD: non-coding RNA activated by DNA damage; TGF-β1: transforming growth factor-β1; RCC2: chromosome condensation 2.

TGF-β1-induced BEAS-2B cells at both transcriptional and translational levels ([Fig. 4F](#) and [G](#)). Downregulation of NORAD caused the suppression of RCC2 expression in TGF-β1-treated BEAS-2B cells, which was restored after RCC2 overexpression ([Fig. 4H](#)). Upregulation of RCC2 not only increased the EMT and migration of TGF-β1-treated BEAS-2B cells, but also reversed the impacts of NORAD knockdown on EMT and cell migration ([Fig. 4I](#) and [J](#)). These results suggested that RCC2 was a target of miR-410-3p and NORAD functioned via mediating RCC2 in TGF-β1-induced BEAS-2B cells.

### 3.5. Knockdown of lncRNA NORAD inactivates Wnt/β-catenin pathway via regulating RCC2

Studies have demonstrated that both NORAD and RCC2 induced EMT via activating the Wnt/β-catenin signaling pathway [[20](#),[33](#)].

Therefore, we further analyzed the influence of NORAD on Wnt/ $\beta$ -catenin pathway in TGF- $\beta$ 1-stimulated BEAS-2B cells. Results showed that TGF- $\beta$ 1 enhanced the expression levels of  $\beta$ -catenin and c-Myc, while the effects were inhibited after NORAD silencing (Fig. 5). However, RCC2 upregulation significantly increased the levels of  $\beta$ -catenin and c-Myc which were suppressed by NORAD downregulation (Fig. 5). These data indicated that knockdown of NORAD inactivated TGF- $\beta$ 1-induced Wnt/ $\beta$ -catenin pathway via regulating RCC2.

3.6. LncRNA NORAD silencing attenuates airway remodeling and EMT in OVA-induced asthmatic model by miR-410-3p/RCC2

The effect of NORAD on asthma was further explored *in vivo* using lentivirus-mediated downregulation of NORAD. As revealed in Fig. 6A, NORAD was increased in the lung tissues of OVA-induced mice, while administration of sh-NORAD lentivirus significantly decreased OVA-induced NORAD in mice. NORAD downregulation decreased lung resistance of asthmatic mice (Fig. 6B). The results of HE and Masson’s staining showed that OVA induced the accumulation of inflammatory cells and collagen deposition in lung tissues. In contrast, knockdown of NORAD attenuated inflammatory infiltration and collagen deposition (Fig. 6C and D). The expression levels of T helper type 2 (Th2) cytokines, such as IL-4 and IL-13, were elevated in OVA-treated mice, but downregulation of NORAD led to their reduction in the serum of asthmatic mice (Fig. 6E and F). Similarly, alteration of serum TGF- $\beta$ 1 levels had the same tendency as Th2 cytokines (Fig. 6G). OVA significantly increased serum total IgE levels, which was suppressed after silencing of NORAD (Fig. 6H). The effect of NORAD on the EMT was further evaluated in asthmatic mice. The expression levels of E-cadherin were suppressed, but N-cadherin levels were enhanced in OVA-treated mice, which were reversed after NORAD knockdown (Fig. 6I). Additionally, the mechanism of NORAD in asthma was confirmed *in vivo*. The results revealed that OVA-treated mice were featured with lower miR-410-3p expression, and higher expression of RCC2,  $\beta$ -catenin and c-Myc than control mice. By contrast, NORAD downregulation significantly increased miR-410-3p, and decreased the expression levels of RCC2,  $\beta$ -catenin and c-Myc in OVA-induced asthmatic mice (Fig. 6I–K). Taken together, these results suggested that silencing of NORAD attenuated airway inflammation and remodeling as well as EMT in OVA-induced asthmatic model via miR-410-3p/RCC2/Wnt/ $\beta$ -catenin pathway.

4. Discussion

Accumulating evidence has indicated that lncRNAs play vital roles in the pathogenesis of asthma [14,34]. LncRNA NORAD has been found to be closely associated with EMT [18,20], an important mechanism underlying airway remodeling in asthma. Suppression of NORAD inhibited inflammatory response in many inflammation-related diseases [35,36]. Whereas, the role of NORAD in asthma remains unreported. For the first time, this study explored the role of NORAD in the pathogenesis of asthma *in vitro* and *in vivo*. Our results found that highly expression of NORAD was exhibited in TGF- $\beta$ 1-induced BEAS-2B cells and OVA-challenged asthmatic mice. Downregulation of NORAD not only suppressed TGF- $\beta$ 1-induced spindle-like morphological changes, migration and proliferation, but also altered the expression of EMT markers in BEAS-2B cells. In OVA-induced asthmatic mouse model, inflammatory cells were aggregated and collagen was deposited in the lungs of mice; moreover, AHR, Th2 cytokines, EMT, serum levels of TGF- $\beta$ 1 and IgE were increased in OVA-induced mice, indicating that mouse asthmatic model was successfully established. Silencing of NORAD dramatically inhibited airway remodeling, including AHR, inflammatory cell infiltration, collagen deposition, EMT, and serum levels of TGF- $\beta$ 1 and

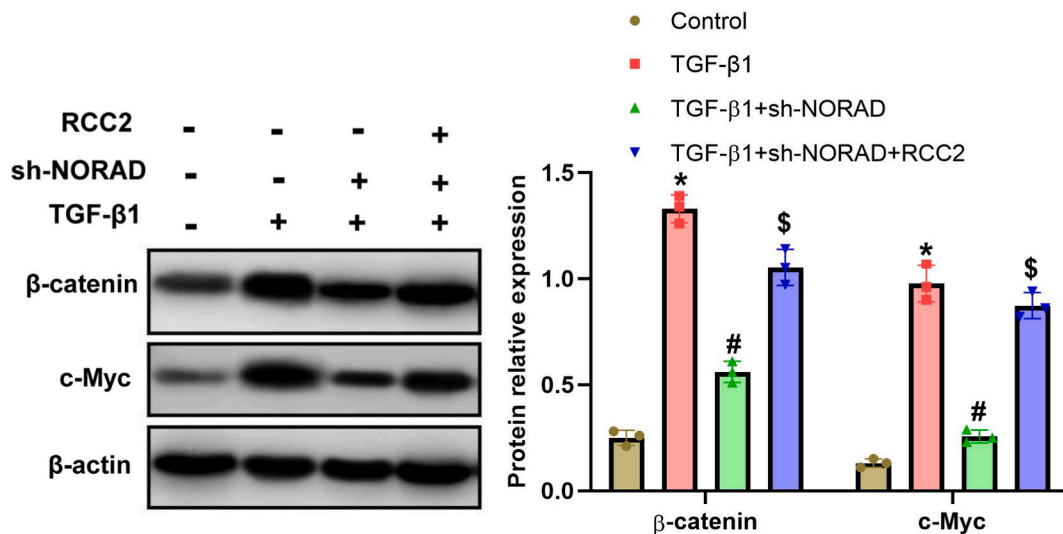
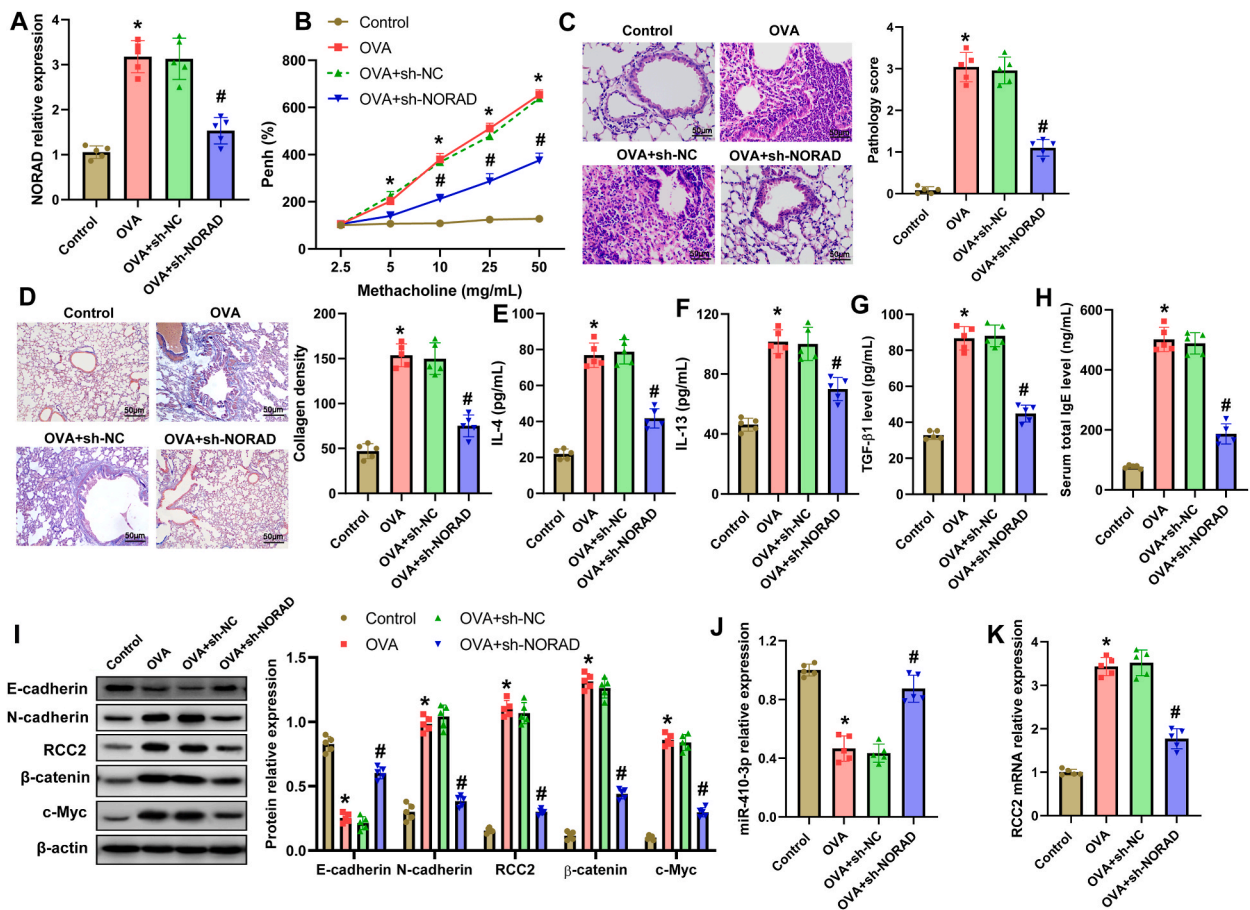


Fig. 5. LncRNA NORAD downregulation inactivated the Wnt/ $\beta$ -catenin pathway via regulating RCC2. The protein levels of  $\beta$ -catenin and c-Myc in TGF- $\beta$ 1-treated BEAS-2B cells that transfected with sh-NORAD or co-transfected with sh-NORAD and RCC2. Non-adjusted images of Western blot analysis were presented in Supplemental Fig. S3. N = 3. \* $P < 0.05$ , compared with the control group; # $P < 0.05$ , compared with the TGF- $\beta$ 1 group; \$ $P < 0.05$ , compared with the TGF- $\beta$ 1+sh-NORAD group. NORAD: non-coding RNA activated by DNA damage; RCC2: chromosome condensation 2.



**Fig. 6.** Silence of lncRNA NORAD attenuated airway inflammation and remodeling as well as EMT in OVA-induced asthmatic model by miR-410-3p/RCC2. **A:** NORAD expression in the lung tissues of mice. **B:** AHR was measured in mice 24 h after the last challenge. **C:** HE staining for the degree of inflammatory cell infiltration. **D:** Masson staining for subepithelial collagen accumulation. Levels of IL-4 (**E**), IL-13 (**F**), TGF- $\beta$ 1 (**G**) and total IgE (**H**) in serum of mice were measured. **I:** Western blot assay for the protein levels of E-cadherin, N-cadherin, RCC2,  $\beta$ -catenin and c-Myc in the lung samples of mice. Non-adjusted images of Western blot analysis were presented in [Supplemental Fig. S4](#). The expression of miR-410-3p (**J**) and RCC2 (**K**) was examined in mouse lungs by qRT-PCR.  $N = 5$ . \* $P < 0.05$ , compared with the control group; # $P < 0.05$ , compared with the OVA group. NORAD: non-coding RNA activated by DNA damage; EMT: epithelial-mesenchymal transition; OVA: ovalbumin; AHR: airway hyper-responsiveness; HE: hematoxylin and eosin; TGF- $\beta$ 1: transforming growth factor- $\beta$ 1; IgE: immunoglobulin E; qRT-PCR: quantitative real-time PCR.

IgE. Also, NORAD knockdown significantly downregulated the secretion of Th2 cytokines like IL-4 and IL-13. Hence, NORAD might be a target for the treatment of asthma.

Previous studies have revealed that miR-410-3p alleviated airway inflammation in OVA-induced asthmatic mice [31,37]. We found that miR-410-3p expression was downregulated by TGF- $\beta$ 1 and suppression of miR-410-3p promoted TGF- $\beta$ 1-induced EMT and migration in BEAS-2B cells. These results suggested that miR-410-3p might inhibit airway remodeling in asthma. Zhang et al. [38] have demonstrated that miR-410-3p was a target of NORAD in neonatal sepsis. In consistent with the report by Zhang et al. [38], this study also confirmed the direct interaction between NORAD and miR-410-3p in asthmatic models. Knockdown of NORAD upregulated miR-410-3p expression both in TGF- $\beta$ 1-induced BEAS-2B cells and in OVA-challenged asthmatic mice. Importantly, miR-410-3p antagonist greatly reversed the influences of NORAD shRNA on the EMT and migration of TGF- $\beta$ 1-induced BEAS-2B cells. Taken together, these results combined with previous reports indicated that NORAD functioned in asthma via directly targeting miR-410-3p.

RCC2 (also known as TD60), a member of RCC1 superfamily, is essential for mitosis [39]. Increasing evidence has shown that RCC2 acted as an oncogene in various cancers, such as colorectal cancer, ovarian cancer, breast cancer, lung adenocarcinoma, and glioma [40,41]. During tumorigenesis, RCC2 induced the EMT in many cancers [33,42]. In this study, RCC2 was highly expressed in TGF- $\beta$ 1-treated BEAS-2B cells and OVA-induced asthmatic mice. And upregulation of RCC2 significantly increased the EMT and migration of TGF- $\beta$ 1-treated BEAS-2B cells. These results demonstrated that RCC2 promoted the EMT in asthma. Studies have demonstrated that RCC2 expression was regulated by miRNAs [43,44]. Bioinformatic analysis indicated that RCC2 was a potential target of miR-410-3p. Dual luciferase reporter assay and RNA pull-down assay verified the sequence-specific binding of miR-410-3p to RCC2. As expected, miR-410-3p dramatically suppressed RCC2 expression in TGF- $\beta$ 1-induced BEAS-2B cells. This indicated that RCC2 was a target of miR-410-3p in asthma. In both asthmatic models, downregulation of NORAD notably inhibited RCC2 expression.

Moreover, upregulation of RCC2 reversed the impacts of NORAD knockdown on the EMT and migration of TGF- $\beta$ 1-induced BEAS-2B cells. These results suggested that NORAD functioned via mediating RCC2 expression in asthma.

NORAD contributed to the EMT progression of prostate cancer via the Wnt/ $\beta$ -catenin pathway [20]. And RCC2 has been demonstrated to induce EMT via activating the Wnt/ $\beta$ -catenin signaling pathway in breast cancer [33]. Wnt/ $\beta$ -catenin signaling is an evolutionarily conserved pathway that regulates various biological activities during embryonic development and adult homeostasis [45]. Aberrant Wnt/ $\beta$ -catenin signaling is related to the pathogenesis of various human diseases, including cancers, metabolic diseases, and inflammatory diseases [37,46]. A previous study has reported that the expression levels of Wnt family proteins and  $\beta$ -catenin were highly expressed in lung samples of asthmatic mice. Blocking  $\beta$ -catenin expression led to the attenuation of airway remodeling [47]. C-Myc is a well-known target gene of Wnt/ $\beta$ -catenin signaling [48]. Therefore, we further analyzed the impact of NORAD on Wnt/ $\beta$ -catenin pathway. Our results showed that NORAD silencing decreased the levels of  $\beta$ -catenin and c-Myc in asthmatic models both *in vitro* and *in vivo*. And RCC2 upregulation abrogated the influence of NORAD downregulation on their expression levels in TGF- $\beta$ 1-induced BEAS-2B cells. These results suggested that silence of NORAD inactivated the Wnt/ $\beta$ -catenin pathway via suppressing RCC2 in asthma. However, this study has some limitations, for example, the expression and mechanism of NORAD are not validated in asthmatic patients, which need further investigation in the future. Additionally, other effect of NORAD on the pathogenesis of asthma except EMT requires more investigation.

## 5. Conclusions

We found that NORAD expression was elevated in asthma. Knockdown of NORAD suppressed EMT-mediated airway remodeling in asthma via sponging miR-410-3p to regulate RCC2 expression, followed by inactivation of the Wnt/ $\beta$ -catenin pathway.

### Animal research ethical approval

All animal experiments were approved by the Animal Care and Use Committee of Henan Children's Hospital (Approval Number: 2021-002).

### Data availability statement

Data will be made available on request from the corresponding author.

### CRedit authorship contribution statement

**Ting Zhang:** Writing – original draft, Project administration, Investigation, Conceptualization. **Han Huang:** Investigation, Conceptualization. **Lihong Liang:** Investigation. **Hongxia Lu:** Investigation, Formal analysis. **Dongge Liang:** Formal analysis.

### Declaration of competing interest

The authors declare that they have no known competing financial interests or personal relationships that could have appeared to influence the work reported in this paper.

### Acknowledgement

This study was supported by the Medical Science and Technology Research Plan Joint Construction Project of Henan Province (LHGJ20200634).

### Abbreviations

AHR	airway hyper-responsiveness
EMT	epithelial-mesenchymal transition
lncRNA	long non-coding RNA
NORAD	non-coding RNA activated by DNA damage
TGF- $\beta$ 1	transforming growth factor- $\beta$ 1
OVA	ovalbumin
ceRNA	competing endogenous RNA
shRNA	short hairpin RNA
qRT-PCR	quantitative real-time PCR
RCC2	chromosome condensation 2
FBS	fetal bovine serum
CCK-8	cell counting kit-8
HE	hematoxylin and eosin
ELISA	enzyme-linked immunosorbent assay

IL	interleukin
IgE	immunoglobulin E
SD	standard deviation
ANOVA	analysis of variance
Th2	T helper type 2

## Appendix A. Supplementary data

Supplementary data to this article can be found online at <https://doi.org/10.1016/j.heliyon.2023.e23860>.

## References

- [1] G. Varricchi, S. Ferri, J. Pepys, R. Poto, G. Spadaro, E. Nappi, et al., Biologics and airway remodeling in severe asthma, *Allergy* 77 (12) (2022) 3538–3552.
- [2] X. Lv, Z. Gao, W. Tang, J. Qin, W. Wang, J. Liu, et al., Trends of therapy in the treatment of asthma, *Ther. Adv. Respir. Dis.* 17 (2023) 17534666231155748.
- [3] A. Tiwari, A.L. Wang, J. Li, S.M. Lutz, A.T. Kho, S.T. Weiss, et al., Seasonal variation in miR-328-3p and let-7d-3p are associated with seasonal allergies and asthma symptoms in children, *Allergy Asthma Immunol Res* 13 (4) (2021) 576–588.
- [4] R. Azmeh, D.E. Greydanus, M.G. Agana, C.A. Dickson, D.R. Patel, M.M. Ischander, et al., Update in pediatric asthma: selected issues, *Dis Mon* 66 (4) (2020) 100886.
- [5] A.L. Devonshire, R. Kumar, *Pediatric asthma: Principles and treatment*, *Allergy Asthma Proc.* 40 (6) (2019) 389–392.
- [6] A. Papi, C. Brightling, S.E. Pedersen, H.K. Reddel, *Asthma*, *Lancet*. 391 (10122) (2018) 783–800.
- [7] P.L. Brand, Inhaled corticosteroids should be the first line of treatment for children with asthma, *Paediatr. Respir. Rev.* 12 (4) (2011) 245–249.
- [8] I. Axelsson, E. Naumburg, S.O. Prietsch, L. Zhang, Inhaled corticosteroids in children with persistent asthma: effects of different drugs and delivery devices on growth, *Cochrane Database Syst. Rev.* 6 (2019) CD010126.
- [9] B.N. Lambrecht, H. Hammad, The immunology of asthma, *Nat. Immunol.* 16 (1) (2015) 45–56.
- [10] K.P. Hough, M.L. Curtiss, T.J. Blain, R.M. Liu, J. Trevor, J.S. Deshane, et al., Airway remodeling in asthma, *Front. Med.* 7 (2020) 191.
- [11] C. Bergeron, W. Al-Ramli, Q. Hamid, Remodeling in asthma, *Proc. Am. Thorac. Soc.* 6 (3) (2009) 301–305.
- [12] Z. Sun, N. Ji, Q. Ma, R. Zhu, Z. Chen, Z. Wang, et al., Epithelial-mesenchymal transition in asthma airway remodeling is regulated by the IL-33/CD146 axis, *Front. Immunol.* 11 (2020) 1598.
- [13] H. He, L. Cao, Z. Wang, Z. Wang, J. Miao, X.M. Li, et al., Sinomenine relieves airway remodeling by inhibiting epithelial-mesenchymal transition through downregulating TGF- $\beta$ 1 and Smad3 expression in vitro and in vivo, *Front. Immunol.* 12 (2021) 736479.
- [14] X. Zhu, Y. Wei, J. Dong, Long noncoding RNAs in the regulation of asthma: Current research and clinical implications, *Front. Pharmacol.* 11 (2020) 532849.
- [15] C. Gu, H. Wang, S. Yang, Diagnostic value of serum long-chain noncoding RNA KCNQ1OT1 in airway remodeling in children with bronchial asthma, *Clin. Lab.* 66 (5) (2020).
- [16] W. Huang, C. Yu, S. Liang, H. Wu, Z. Zhou, A. Liu, et al., Long non-coding RNA TUG1 promotes airway remodeling and mucus production in asthmatic mice through the microRNA-181b/HMGB1 axis, *Int. Immunopharm.* 94 (2021) 107488.
- [17] S. Lee, F. Kopp, T.C. Chang, A. Sataluri, B. Chen, S. Sivakumar, et al., Noncoding RNA NORAD regulates genomic stability by sequestering PUMILIO proteins, *Cell* 164 (1–2) (2016) 69–80.
- [18] H. Li, X. Wang, C. Wen, Z. Huo, W. Wang, Q. Zhan, et al., Long noncoding RNA NORAD, a novel competing endogenous RNA, enhances the hypoxia-induced epithelial-mesenchymal transition to promote metastasis in pancreatic cancer, *Mol. Cancer* 16 (1) (2017) 169.
- [19] N. Kawasaki, T. Miwa, S. Hokari, T. Sakurai, K. Ohmori, K. Miyauchi, et al., Long noncoding RNA NORAD regulates transforming growth factor- $\beta$  signaling and epithelial-to-mesenchymal transition-like phenotype, *Cancer Sci.* 109 (7) (2018) 2211–2220.
- [20] Y. Zhang, Y. Li, Long non-coding RNA NORAD contributes to the proliferation, invasion and EMT progression of prostate cancer via the miR-30a-5p/RAB11A/WNT/ $\beta$ -catenin pathway, *Cancer Cell Int.* 20 (1) (2020) 571.
- [21] Y. Itoigawa, N. Harada, S. Harada, Y. Katsura, F. Makino, J. Ito, et al., TWEAK enhances TGF- $\beta$ -induced epithelial-mesenchymal transition in human bronchial epithelial cells, *Respir. Res.* 16 (2015) 48.
- [22] J. Zhu, L. Wang, The role of lncRNA-miR-26a-mRNA network in cancer progression and treatment, *Biochem. Genet.* (2023), <https://doi.org/10.1007/s10528-023-10475-w>.
- [23] M. Taheri, A. Safarzadeh, B.M. Hussien, S. Ghafouri-Fard, A. Baniahmad, lncRNA/miRNA/mRNA network introduces novel biomarkers in prostate cancer, *Cells* 11 (23) (2022).
- [24] Y. Song, Z. Wang, J. Jiang, Y. Piao, L. Li, C. Xu, et al., DEK-targeting aptamer DTA-64 attenuates bronchial EMT-mediated airway remodelling by suppressing TGF- $\beta$ 1/Smad, MAPK and PI3K signalling pathway in asthma, *J. Cell Mol. Med.* 24 (23) (2020) 13739–13750.
- [25] T.W. Flanagan, M.N. Sebastian, D.M. Battaglia, T.P. Foster, S.A. Cormier, C.D. Nichols, 5-HT<sub>2</sub> receptor activation alleviates airway inflammation and structural remodeling in a chronic mouse asthma model, *Life Sci.* 236 (2019) 116790.
- [26] Y.L. Chen, B.L. Chiang, Targeting TSLP with shRNA alleviates airway inflammation and decreases epithelial CCL17 in a murine model of asthma, *Mol. Ther. Nucleic Acids* 5 (2016) e316.
- [27] W.C. Huang, C.Y. Liu, S.C. Shen, L.C. Chen, K.W. Yeh, S.H. Liu, et al., Protective effects of Licochalcone A improve airway hyper-responsiveness and oxidative stress in a mouse model of asthma, *Cells* 8 (6) (2019) 617.
- [28] F.Q. Zhang, X.P. Han, F. Zhang, X. Ma, D. Xiang, X.M. Yang, et al., Therapeutic efficacy of a co-blockade of IL-13 and IL-25 on airway inflammation and remodeling in a mouse model of asthma, *Int. Immunopharm.* 46 (2017) 133–140.
- [29] N. Landeros, P.M. Santoro, G. Carrasco-Avino, A.H. Corvalan, Competing endogenous RNA networks in the epithelial to mesenchymal transition in diffuse-type of gastric cancer, *Cancers* 12 (10) (2020) 2741.
- [30] J. Behera, A. Kumar, M.J. Voor, N. Tyagi, Exosomal lncRNA-H19 promotes osteogenesis and angiogenesis through mediating Angpt1/Tie2-NO signaling in CBS-heterozygous mice, *Theranostics* 11 (16) (2021) 7715–7734.
- [31] R. Jin, S. Hu, X. Liu, R. Guan, L. Lu, R. Lin, Intranasal instillation of miR410 targeting IL4/IL13 attenuates airway inflammation in OVA-induced asthmatic mice, *Mol. Med. Rep.* 19 (2) (2019) 895–900.
- [32] L. Zhang, Y. Pang, X. Cui, W. Jia, W. Cui, Y. Liu, et al., MicroRNA-410-3p upregulation suppresses proliferation, invasion and migration, and promotes apoptosis in rhabdomyosarcoma cells, *Oncol. Lett.* 18 (1) (2019) 936–943.
- [33] Z. Chen, W. Wu, Y. Huang, L. Xie, Y. Li, H. Chen, et al., RCC2 promotes breast cancer progression through regulation of Wnt signaling and inducing EMT, *J. Cancer* 10 (27) (2019) 6837–6847.
- [34] Z. Chen, N. Fan, G. Shen, J. Yang, Silencing lncRNA CDKN2B-AS1 alleviates childhood asthma progression through inhibiting ZFP36 promoter methylation and promoting NR4A1 expression, *Inflammation* 46 (2) (2023) 700–717.
- [35] D.N. Fu, Y. Wang, L.J. Yu, M.J. Liu, D. Zhen, Silenced long non-coding RNA activated by DNA damage elevates microRNA-495-3p to suppress atherosclerotic plaque formation via reducing Kruppel-like factor 5, *Exp. Cell Res.* 401 (2) (2021) 112519.

- [36] S. Zhou, D. Zhang, J. Guo, Z. Chen, Y. Chen, J. Zhang, Long non-coding RNA NORAD functions as a microRNA-204-5p sponge to repress the progression of Parkinson's disease in vitro by increasing the solute carrier family 5 member 3 expression, *IUBMB Life* 72 (9) (2020) 2045–2055.
- [37] N. Tong, D. Liu, L. Lu, R. Lin, R. Jin, miR-410 regulates helper T cell differentiation in ovalbumin-induced asthma through the PI3K-AKT-VEGF signaling pathway, *Int. Arch. Allergy Immunol.* (2023) 1–9.
- [38] H. Zhang, L. Li, L. Xu, Y. Zheng, Clinical significance of the serum lncRNA NORAD expression in patients with neonatal sepsis and its association with miR-410-3p, *J. Inflamm. Res.* 14 (2021) 4181–4188.
- [39] X. Li, K. Kang, Y. Peng, L. Shen, L. Shen, Y. Zhou, Comprehensive analysis of the expression profile and clinical implications of regulator of chromosome condensation 2 in pan-cancers, *Aging (Albany NY)* 14 (22) (2022) 9221–9242.
- [40] K. Guo, C. Zhao, B. Lang, H. Wang, H. Zheng, F. Zhang, Regulator of Chromosome Condensation 2 modulates cell cycle progression, tumorigenesis, and therapeutic resistance, *Front. Mol. Biosci.* 7 (2020) 620973.
- [41] T. Liu, Y. Wang, Y. Wang, S.K. Cheung, P.M. Or, C.W. Wong, et al., The mitotic regulator RCC2 promotes glucose metabolism through BACH1-dependent transcriptional upregulation of hexokinase II in glioma, *Cancer Lett.* 549 (2022) 215914.
- [42] B. Pang, N. Wu, R. Guan, L. Pang, X. Li, S. Li, et al., Overexpression of RCC2 enhances cell motility and promotes tumor metastasis in lung adenocarcinoma by inducing epithelial-mesenchymal transition, *Clin. Cancer Res.* 23 (18) (2017) 5598–5610.
- [43] X. Xu, X. Zhou, J. Zhang, H. Li, Y. Cao, X. Tan, et al., MicroRNA-191 modulates cisplatin-induced DNA damage response by targeting RCC2, *FASEB J* 34 (10) (2020) 13573–13585.
- [44] M. Matsuo, C. Nakada, Y. Tsukamoto, T. Noguchi, T. Uchida, N. Hijiya, et al., MiR-29c is downregulated in gastric carcinomas and regulates cell proliferation by targeting RCC2, *Mol. Cancer* 12 (2013) 15.
- [45] M. Hussain, C. Xu, M. Lu, X. Wu, L. Tang, X. Wu, Wnt/ $\beta$ -catenin signaling links embryonic lung development and asthmatic airway remodeling, *Biochim. Biophys. Acta, Mol. Basis Dis.* 1863 (12) (2017) 3226–3242.
- [46] H. Clevers, R. Nusse, Wnt/ $\beta$ -catenin signaling and disease, *Cell* 149 (6) (2012) 1192–1205.
- [47] H.J. Kwak, D.W. Park, J.Y. Seo, J.Y. Moon, T.H. Kim, J.W. Sohn, et al., The Wnt/ $\beta$ -catenin signaling pathway regulates the development of airway remodeling in patients with asthma, *Exp. Mol. Med.* 47 (2015) e198.
- [48] F. Wu, T. Xing, X. Gao, F. Liu, miR-501-3p promotes colorectal cancer progression via activation of Wnt/ $\beta$ -catenin signaling, *Int. J. Oncol.* 55 (3) (2019) 671–683.